Acta Oceanol. Sin., 2023, Vol. 42, No. 5, P. 154–165
https://doi.org/10.1007/s13131-022-2065-6
http://www.aosocean.com
E-mail: ocean2@hyxb.org.cn

Shallow water bathymetry based on a back propagation neural network and ensemble learning using multispectral satellite imagery

Sensen Chu[1, 2, 3], Liang Cheng[1, 2, 3, 4*], Jian Cheng[1, 3], Xuedong Zhang[1, 3], Jie Zhang[5], Jiabing Chen[5], Jinming Liu[6*]

[1] Jiangsu Provincial Key Laboratory of Geographic Information Science and Technology, Nanjing University, Nanjing 210023, China

[2] Collaborative Innovation Center of South China Sea Studies, Nanjing University, Nanjing 210093, China

[3] School of Geography and Ocean Science, Nanjing University, Nanjing 210023, China

[4] Jiangsu Center for Collaborative Innovation in Novel Software Technology and Industrialization, Nanjing 210023, China

[5] Zhejiang Institute of Hydraulics and Estuary, Hangzhou 310020, China

[6] Institute of Defense Engineering, Academy of Military Sciences, Beijing 100036, China

Received 5 December 2021; accepted 12 June 2022

Abstract

The back propagation (BP) neural network method is widely used in bathymetry based on multispectral satellite imagery. However, the classical BP neural network method faces a potential problem because it easily falls into a local minimum, leading to model training failure. This study confirmed that the local minimum problem of the BP neural network method exists in the bathymetry field and cannot be ignored. Furthermore, to solve the local minimum problem of the BP neural network method, a bathymetry method based on a BP neural network and ensemble learning (BPEL) is proposed. First, the remote sensing imagery and training sample were used as input datasets, and the BP method was used as the base learner to produce multiple water depth inversion results. Then, a new ensemble strategy, namely the minimum outlying degree method, was proposed and used to integrate the water depth inversion results. Finally, an ensemble bathymetric map was acquired. Anda Reef, northeastern Jiuzhang Atoll, and Pingtan coastal zone were selected as test cases to validate the proposed method. Compared with the BP neural network method, the root-mean-square error and the average relative error of the BPEL method can reduce by 0.65–2.84 m and 16%–46% in the three test cases at most. The results showed that the proposed BPEL method could solve the local minimum problem of the BP neural network method and obtain highly robust and accurate bathymetric maps.

Key words: bathymetry, back propagation neural network, ensemble learning, local minimum problem, multispectral satellite imagery

Citation: Chu Sensen, Cheng Liang, Cheng Jian, Zhang Xuedong, Zhang Jie, Chen Jiabing, Liu Jinming. 2023. Shallow water bathymetry based on a back propagation neural network and ensemble learning using multispectral satellite imagery. Acta Oceanologica Sinica, 42(5): 154–165, doi: 10.1007/s13131-022-2065-6

1 Introduction

Shallow water bathymetric maps constitute important geographical data that have a wide range of applications in coastal management (Sun et al., 2021), sailing safety (Andréfouët et al., 2003), reef island construction (Andrejev et al., 2011), and coral reef ecosystems (Melet et al., 2020). Traditionally, shallow water bathymetric data are collected using ship-mounted acoustic and airborne light detection and ranging. However, these approaches are expensive and impractical in sensitive areas (Wang et al., 2020). In recent years, multispectral satellite imagery (MSI)-based bathymetric methods have received much attention because of their advantages, including low cost, wide coverage, rich data sources, and no region restriction (Casal et al., 2019; Cao et al., 2021).

The MSI-based bathymetric methods originated in the 1970s (Polcyn, 1976). Through decades of bathymetric theory development, many classical MSI-based bathymetric methods have been proposed, such as the theoretical analysis method (Lee et al., 1998; Huang et al., 2017), Stumpf band ratio method (Stumpf et al., 2003; Leon and Cohen, 2012; Ma et al., 2020), Lyzenga polynomial method (Lyzenga, 1978, 1985; Liang et al., 2017; Manessa et al., 2018), and back propagation (BP) neural network method (Sandidge and Holyer, 1998; Liu et al., 2018; Collin et al., 2017). Among these methods, the BP neural network method (hereinafter referred to BP method) has exhibited the best inversion performance in many studies and is widely used in recent years (Ceyhun and Yalçın, 2010; Gholamalifard et al., 2013; Liu et al., 2015; Chu et al., 2019; Guo et al., 2021). The BP method has been

Foundation item: The National Natural Science Foundation of China under contract No. 42001401; the China Postdoctoral Science Foundation under contract No. 2020M671431; the Fundamental Research Funds for the Central Universities under contract No. 0209-14380096; the Guangxi Innovative Development Grand Grant under contract No. 2018AA13005.
*Corresponding author, E-mail: lcheng@nju.edu.cn; Liujm1025@outlook.com

applied by many authors in different types of environments using data from different satellites, including Landsat-8 (El-Mewafi et al., 2018), Sentinel-2 (Chu et al., 2019), Quickbird (Ceyhun and Yalçın, 2010), Spot-6 (Hussein and Nadaoka, 2017), and WorldView-3 (Collin et al., 2017).

The BP method is a feedforward neural network with error backpropagation and is one of the most widely applied neural network models (Li et al., 2012). The BP method was proposed by a group of scientists lead by Rumelhart and McCelland in 1986 (Rumelhart and McClelland, 1986). Subsequently, the Stennis Space Center of the Naval Research Laboratory used the BP method for shallow water bathymetry (Sandidge and Holyer, 1998), using the following processes. First, the spectral reflectance and water depth data are the input and output layers, respectively. Second, the weighting matrix of the hidden layer was corrected by measured water depth. Finally, the corrected model was used for water depth inversion. MSI-based bathymetry is affected by numerous variables, including seafloor sediments, water chlorophyll, atmospheric aerosols, and solar altitude. These features determine the nonlinearity of water depth inversion (Ceyhun and Yalçın, 2010). The greatest advantage of the BP method is its excellent nonlinear fitting ability (Qiu et al., 2018; Kim et al., 2019), which is why the BP method is superior to others in many studies. Another advantage of the BP method is its ease of use because the user does not need to understand the physical model of water depth inversion and can train the inversion model directly using sample data. Therefore, the BP method has been widely employed.

However, the classical BP method easily falls into a local minimum (Hirose et al., 1991; Deng et al., 2021). The BP method adopts a decreasing gradient algorithm to determine the optimal solution, and the error function is a curved multi-dimensional space, which, in the training process, may fall into a small valley area and generate local minima, leading to model training failure (Lee et al., 1993). In theory, the local minimum problem can be solved by selecting appropriate parameters (such as the learning rate and the number of hidden layer nodes) and the initial network weight. The appropriate parameters can be selected by empirical and traversal methods (Islam et al., 2003; Benardos and Vosniakos, 2007). However, the initial network weight is difficult to set manually because of the large quantity; thus, the random assignment method is commonly adopted. Therefore, it is random and unruly that the BP method falls into the local minimum.

The shallow water bathymetry based on the BP method also faces the same problem of local minima. In order to avoid the problem, researchers usually contrast bathymetry results with measured water depth samples and then estimate the problem of local minima depending on the artificial experience. If the local minima are suspected, researchers must produce a new bathymetry result by changing the initial network weight of the BP method and reestimate it. This process is subjective and inconvenient. Therefore, shallow water bathymetry based on the BP method is discussed and improved through experimental research. The main contributions of this paper are that a bathymetry method based on a BP neural network and ensemble learning is proposed, which solves the local minimum problem of the BP method.

2 Bathymetry method based on a BP neural network and ensemble learning

In this paper, we propose a bathymetry method based on a BP neural network and ensemble learning (BPEL). As shown in Fig. 1, the remote sensing imagery and training sample are the input dataset, and the BP method is used as the base learner to produce multiple water depth inversion results. Then, a new ensemble strategy, the minimum outlying degree method, is proposed and used to integrate the water depth inversion results. Finally, an ensemble bathymetric map is acquired.

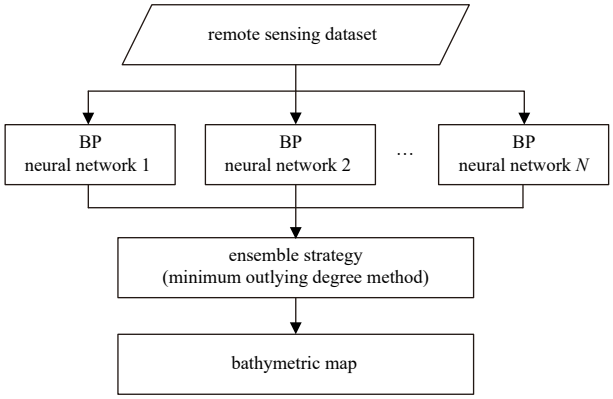

Fig. 1. Procedures of bathymetry method based on a back propagation (BP) neural network and ensemble learning.

2.1 *Base learner: BP neural network*

The BP method is expressed as

$$\begin{cases} \boldsymbol{H} = f(w\boldsymbol{X} + \theta_H) \\ \boldsymbol{O} = f(v\boldsymbol{H} + \theta_o) \end{cases}, \tag{1}$$

where $\boldsymbol{X}$, $\boldsymbol{H}$, and $\boldsymbol{O}$ are the input layer, hidden layer, and output layer vectors, respectively; w and v are the weight vectors of connections from the input layer to the hidden layer and from the hidden layer to the output layer, respectively; and θ_H and θ_o are the activation thresholds of the neural elements in the hidden layer and output layer, respectively. Function f is usually a nonlinear sigmoidal function applied to the weighted sum of inputs before the signal passes to the next layer. During the learning processes of a BP neural network, a squared error, such as $E = \frac{1}{2}\sum(\boldsymbol{O} - \boldsymbol{O}_o)^2$, is usually used as the error function, where $\boldsymbol{O}_o$ is the expected output vector.

2.2 *Ensemble strategy: minimum outlying degree method*

Because the initial network weight of the base learner BP neural network is randomly different, each base learner will produce a water depth inversion result, that is, a water depth set $S = \{d_1, d_2, \cdots, d_l, \cdots, d_L\}$ in the same geographical location, where L is the number of base learners, and d_l represents the water depth from the inversion of the lth-base learner. To integrate the water depth set S, we propose an ensemble strategy based on the minimum outlying degree. The outlying degree is expressed as

$$OD_l = \frac{1}{L-1}\sum_{i=1,\ i\neq l}^{L} |d_l - d_i|, \tag{2}$$

where OD_l is the outlying degree of the water depth result d_l, the range of OD_l is [0, 1]; the greater the OD_l, the greater is the likelihood that d_l is noise. It should be noted that the OD_l is valid only when $L \geqslant 2$. The procedures of the ensemble strategy are based on the minimum outlying degree, as shown in Fig. 2.

(1) Calculating the outlying degree of each water depth result in S: According to Eq. (2), the outlying degree of the water depth set $S = \{d_1, d_2, d_3, \cdots, d_L\}$ is $\{OD_1, OD_2, OD_3, \cdots, OD_L\}$.

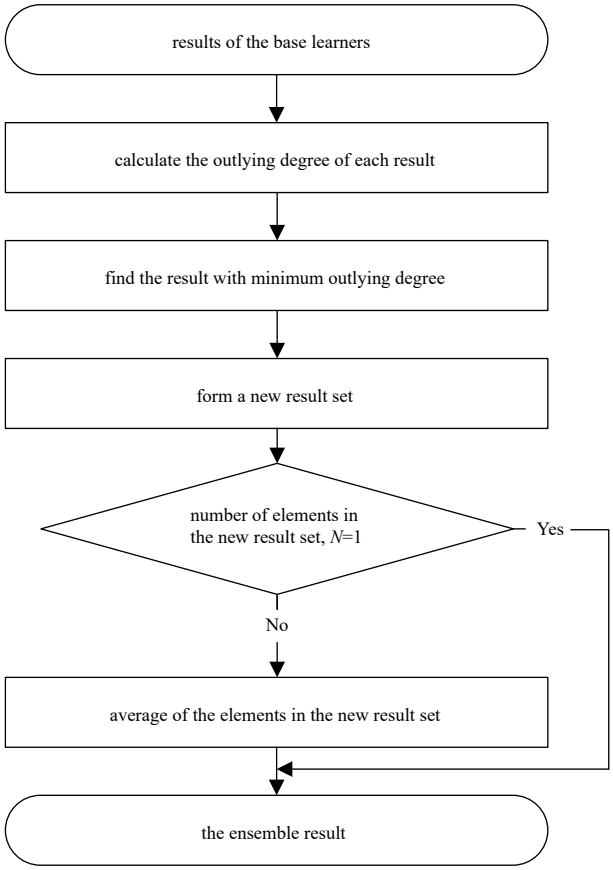

Fig. 2. Procedures of the ensemble strategy based on the minimum outlying degree.

(2) Finding the water depth results with the minimum outlying degree: The minimum outlying degree OD_p and corresponding number p were determined by $OD_p = \min\{OD_1, OD_2, OD_3, \cdots, OD_L\}$, $p \in \{1, 2, 3, \cdots, L\}$. Then, the water depth results d_p, which have a minimum outlying degree, are formed into a new water depth set $S' = \{d_p\}$. It should be noted that the p and d_p maybe unique or multiple, because the final minimum outlying degree maybe has two or more identical values.

(3) Averaging the element of S': When the number of elements in the new water depth set S' is N=1, the d_p is the ensemble result. When N>1, the average of elements in S' is the ensemble result.

(4) Traversing the entire experimental area: The ensemble bathymetric map was acquired by traversing the entire experimental area.

2.3 *Result evaluation*

The accuracy assessment was performed using two statistical parameters: the root-mean-square error (RMSE) and the average relative error (ARE). The smaller the RMSE and ARE values, the higher the accuracy of the bathymetric inversion.

$$\mathrm{RMSE} = \sqrt{\sum_{i=1}^{n} \frac{(z_i - \widehat{z}_i)^2}{n}}, \tag{3}$$

$$\mathrm{ARE} = \frac{1}{n} \sum_{i=1}^{n} \frac{|z_i - \widehat{z}_i|}{z_i}, \tag{4}$$

where z_i is the measured water depth, $\widehat{z}_i$ is the inverted water depth, and n is the number of test samples.

3 Experiments and analysis

3.1 *Study area and data*

The study areas were the Anda Reef (Fig. 3a), northeastern Jiuzhang Atoll (Fig. 3b), and Pingtan coastal zone (Fig. 3c). The water bodies in Anda Reef and northeastern Jiuzhang Atoll are oceanic waters (CASE I waters), and the water body in Pingtan coastal zone is CASE II waters.

The MSIs were acquired using Sentinel-2 satellites. The Level-1C product is used for bathymetric inversion. The acquired times of MSIs for the Anda Reef (Fig. 3a), northeastern Jiuzhang Atoll (Fig. 3b), and Pingtan coastal zone (Fig. 3c) were April 9, 2017 (02:35 universal time coordinated (UTC)), March 15, 2018 (02:35 UTC), and February 22, 2021 (02:37 UTC), respectively. The image coordinate system of Anda Reef, northeastern Jiuzhang Atoll, and Pingtan coastal zone were WGS84 UTM 49N, WGS84 UTM 49N, and WGS84 UTM 50N, respectively. The bands of Sentinel-2 MSIs used in this study were blue, green, and red, with a resolution of 10 m. The digital number (DN) values of these bands are the input layers of the neural network.

The *in situ* depth data of the Anda Reef (Fig. 3a), northeastern Jiuzhang Atoll (Fig. 3b), and Pingtan coastal zone (Fig. 3c) were measured by the Odom Hydrotrac II (Teledyne Odom Hydrographic, Baton Rouge, LA, USA) single-beam and SONIC 2024 (R2Sonic LLC, Austin, TX, USA) multibeam echo sounders. Both have a depth accuracy of 0.01 m. An Applanix POS MV Elite (Trimble, Inc., Sunnyvale, CA, USA) position and orientation system was used to provide positional data, and we also used the Fugro Marinestar (Fugro N.V., Leidschendam, the Netherlands) satellite-based positioning service, which has a horizontal positioning accuracy of 0.1 m and a vertical positioning accuracy of 0.15 m. The depth datum was referenced to the mean sea level (MSL). The MSL of the Anda Reef, northeastern Jiuzhang Atoll, and Pingtan coastal zone are 1.30 m, 1.30 m, and 4.03 m above the tidal datum, respectively. The tidal levels of image acquisition time of the Anda Reef, northeastern Jiuzhang Atoll, and Pingtan coastal zone are 1.39 m, 1.13 m, and 3.90 m, respectively. Depth measurements were corrected to the instantaneous depth of image acquisition time, and the coordinate systems are identical to the MSIs. We calculated the mean depth values within each image pixel. The 1 315 pixels in the Anda Reef contain depth data, and depths ranged from 0 m to 20 m. The 1 321 pixels in the northeastern Jiuzhang Atoll contain depths ranging from 0 m to 30 m. The 1 185 pixels in the Pingtan coastal zone contain depths ranging from 0 m to 5 m.

3.2 *Comparison of the robustness of the BP and BPEL methods*

In this section, we compare the robustness of the BP and BPEL methods. The BP method was implemented using MATLAB, and the experimental setup refers to the literature (Chu et al., 2019) which has excellent inversion performance, specifically as follows. The input layer contained three nodes (red, green, and blue bands), and the hidden layer contained seven nodes. The transfer functions in the hidden and output layers were tansig and purelin, respectively, and the training function was trainlm. The maximum number of trainings, learning rate, momentum factor, and training target error were 1 500, 0.05, 0.9, and 10^{-5}, respectively. The experimental setup of the BPEL method was as follows. There were five base learners, and the setup of the base learner was identical to that of the BP method. Three hun-

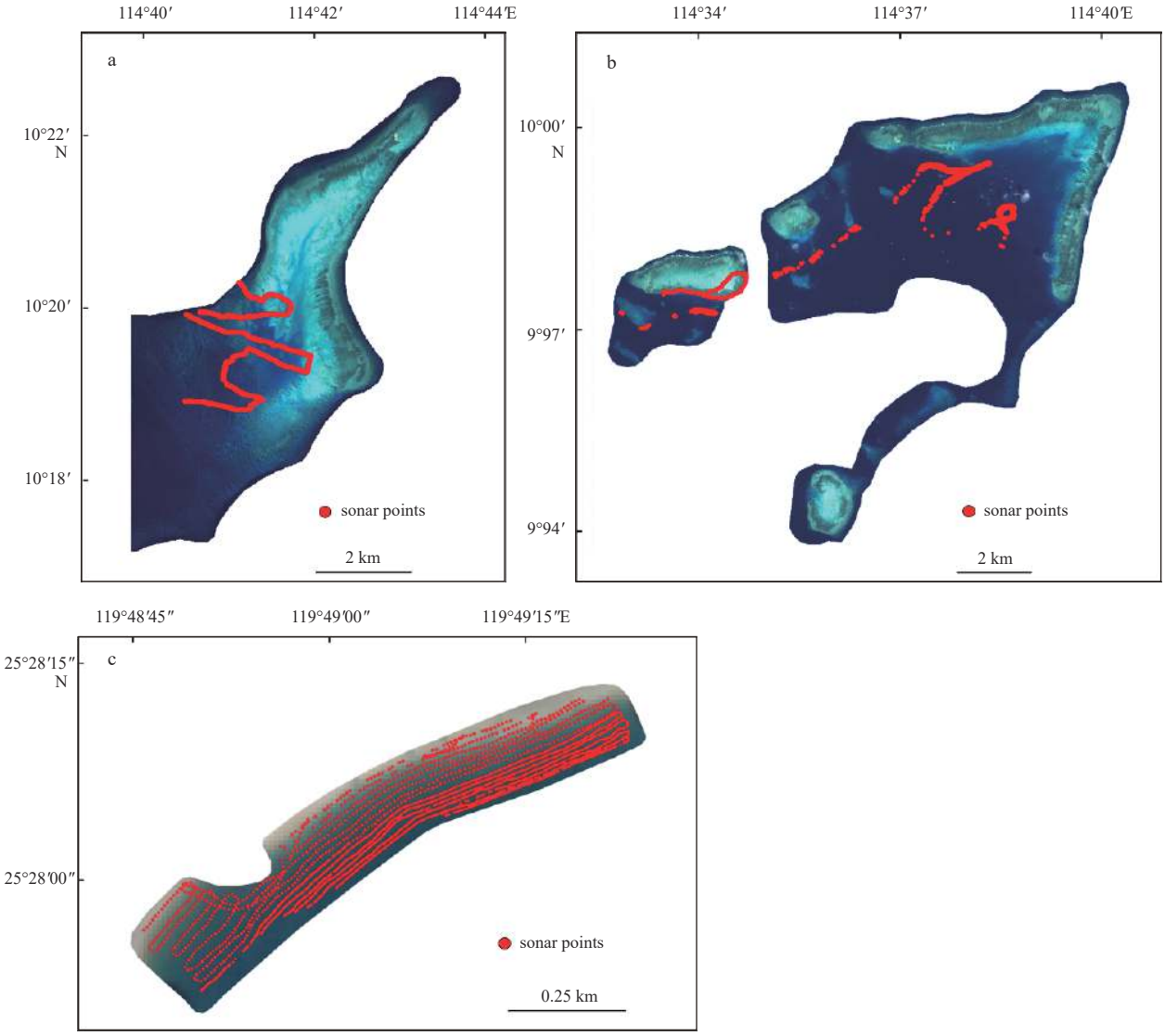

Fig. 3. Study areas and data for the Anda Reef (a), northeastern Jiuzhang Atoll (b), and Pingtan coastal zone (c).

dred pixels that contained depth data were randomly selected as training samples, and the remaining pixels were used as test samples. The BP and BPEL methods shared a set of training and test samples. To compare the robustness of the BP and BPEL methods, 100 repeated experiments were performed for the two methods. The RMSEs of 100 repeated experiments using the BP and BPEL methods are compared in Fig 4. Figure 4 shows that the RMSEs of the BP method are scattered and have poor robustness, whereas the RMSEs of the BPEL method are stable and robust.

3.3 *Comparison of bathymetric maps of BP and BPEL methods*

There is a great variation of the robustness between the BP and BPEL methods, though the best results of both methods are outstanding and similar (Figs 4 and A1). In this section, the three worst results in the 100 repeated experiments (Fig. 4), which are representative of the BP and BPEL methods, are compared to analyze the difference between the two methods. In the Anda Reef experiment, the three worst results, in order, of the BP method, were the 85th, 31st, and 91st repeated experiments. The three worst results, in order, of the BPEL method were the 50th, 70th, and 96th repeated experiments. The bathymetric maps of the three worst results of the BP and BPEL methods are compared in Fig. 5, and their error scatterplots are compared in Fig. 6. In the northeastern Jiuzhang Atoll experiment, the three worst results of the BP method, in order, were the 57th, 72nd, and 91st repeated experiments. The three worst results of the BPEL method, in order, were the 96th, 58th, and 8th repeated experiments. The bathymetric maps of the three worst results of the BP and BPEL methods are compared in Fig. 7, and their error scatterplots are compared in Fig. 8. In the Pingtan coastal zone experiment, the three worst results of the BP method, in order, were the 41st, 39th, and 45th repeated experiments. The three worst results of the BPEL method, in order, were the 43rd, 74th, and 59th repeated experiments. The bathymetric maps of the three worst results of the BP and BPEL methods are compared in Fig. 9, and their error scatterplots are compared in Fig. 10. Table 1 compared the inversion accuracies (RMSEs) of the three worst results of the BP and BPEL method in the Anda Reef, northeastern Jiuzhang Atoll, and Pingtan coastal zone.

In Fig. 5, the bathymetric maps of the BP method on the southwest corner of the Anda Reef are shallower than the real values and lose many underwater terrain features (Figs 5a–c). On the northeast corner of the Anda Reef, the bathymetric maps of

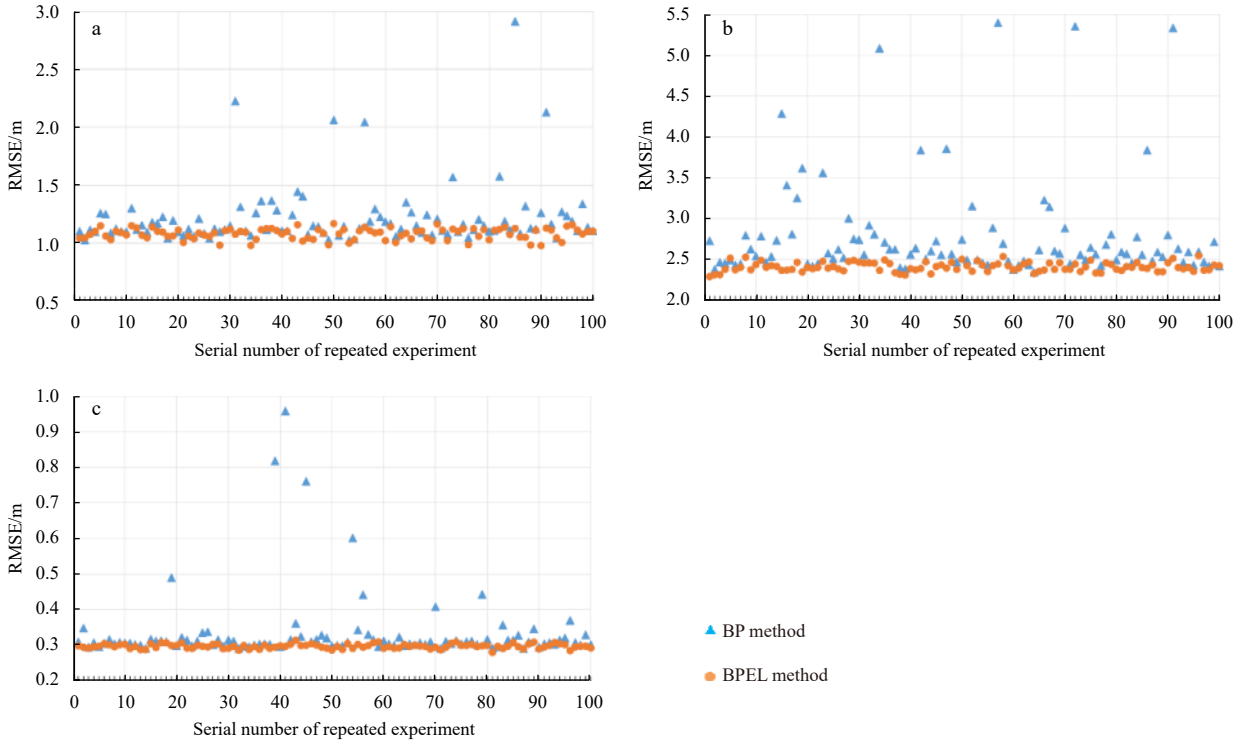

Fig. 4. Root-mean-square errors (RMSEs) of 100 repeated experiments of the back propagation (BP) and BP neural network and ensemble learning (BPEL) methods for the Anda Reef (a) northeastern Jiuzhang Atoll (b) and Pingtan coastal zone (c).

the BP method are deeper than the real values, and the coral reef contours are indistinct (Figs 5a–c). In Fig. 7, the bathymetric maps of the BP method exhibit large differences. Figures 7a and b are also shallower than the real values and lose many underwater terrain features in the blue-colored deep-water region. Figure 7c mistakenly retrieved the red-colored shallow water reefs as blue-colored deep-water regions. In Fig. 9, the bathymetric maps of the BP method also exhibit large differences. Figure 9a is shallower than the real values in the southeast, and Figs 9b and c have lots of speckle noise. Compared with the BP method, the bathymetric maps of BPEL were stable and had clear coral reef contours (Figs 5d–f, 7d–f, and 9d–f).

Figures 6, 8, 10, and Table 1 quantitatively display the superiority of the BPEL method. The correlations between estimated depth versus measured depth in the BPEL method are significantly higher than those in the BP method (Figs 6, 8, and 10). The RMSE and ARE of the BPEL method were 0.99–1.76 m, 12%–16% lower than those of the BP method in the Anda Reef experiment. The RMSE and ARE of the BPEL method were 2.80–2.84 m, 35%–46% lower than those of the BP method in the northeastern Jiuzhang Atoll experiment. The RMSE and ARE of the BPEL method were 0.46–0.65 m, 2%–26% lower than those of the BP method in the Pingtan coastal zone experiment. From the view of different depths of water, the RMSEs of the BPEL method all are lower than those of the BP method (Table 1). In summary, there were many errors in the inversion results of the traditional BP method, whereas the proposed BPEL method was superior to the BP method in terms of bathymetric maps and inversion accuracy.

3.4 *Effects of the number of training samples on BPEL methods*

To study the effects of the number of training samples K on the BP and BPEL methods, we varied K between 5 and 1 000 in intervals of 5. We set up 10 repeated experiments for each value of K, and the average RMSE of the 10 repeated experiments was used as the inversion accuracy of the number of training samples K. In addition to K, the other parameters of the BP and BPEL methods were identical to the experiments in Section 3.2. Figure 11 shows the effects of training samples K on the BP and BPEL methods; the error bars represent the standard deviations of the 10 RMSE values. In Fig. 11, the RMSE of the bathymetric inversion initially decreases and then stabilizes as K increases. However, in the plateau stage of RMSE (K>200), the accuracy of the BPEL method was superior to that of the BP method, and the error bars of the BPEL method were negligible.

3.5 *Effects of the number of base learners on BPEL methods*

Compared with the BP method, the proposed BPEL method adds a new parameter: the number of base learners, L. To study the impact on the inversion accuracy of the BPEL method, we varied L between 2 and 20 in intervals of 1. As a contrast, the inversion accuracy of the BP method was calculated and was shown at the place L=1 (because the mathematical model of the BP method has one base learner). We also set up 10 repeated experiments for each value of L, and the average RMSE of the 10 repeated experiments was used as the inversion accuracy of the number of L. In addition to L, the other parameters of the BPEL and BP methods were identical to the experiments in Section 3.2. The effects of the number of base learners L on the BPEL methods are shown in Fig. 12, with the error bars representing the standard deviation of the 10 RMSE values. From Fig. 12, the variation in RMSE with increasing L had two distinct phases. In the first phase, the RMSE decreases, but the error bars are still very large when L<3. In the second phase, the RMSE is stable, and the error bars are very small when $L\geqslant 3$. In addition, compared with the RMSEs of the BP method, the RMSEs of the BPEL method are lower and more robust when $L\geqslant 3$.

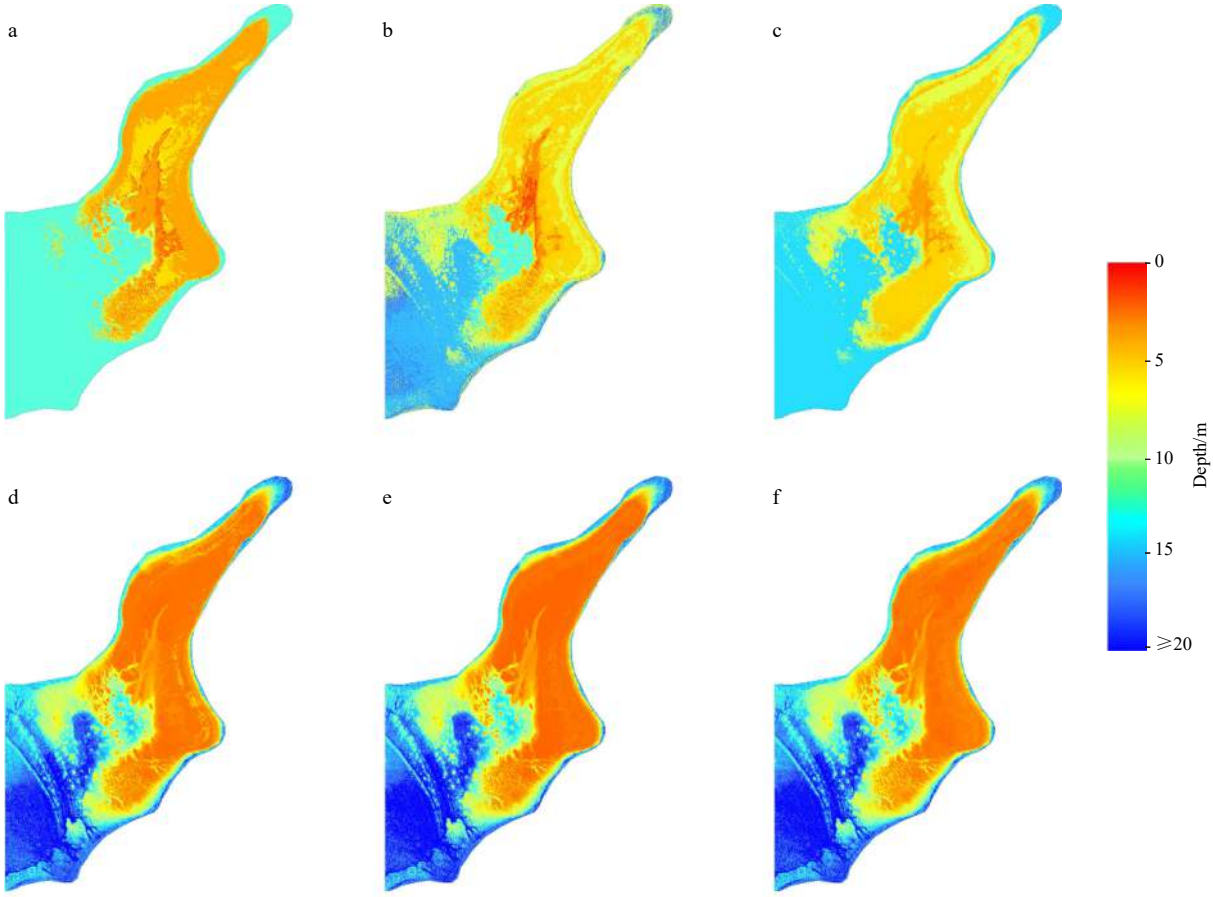

Fig. 5. Bathymetric maps of the three worst results for the back propagation (BP) and BP neural network and ensemble learning (BPEL) methods in the Anda Reef. a–c. Bathymetric maps of the 85th, 31st, and 91st repeated experiments for the BP method. d–f. Bathymetric maps of the 50th, 70th, and 96th repeated experiments for the BPEL method.

4 Discussion

4.1 *Performance advantages of the BPEL method compared with the BP method*

The BP method was not robust. Although the BP method can obtain a high-accuracy bathymetric map in most cases, a bathymetric map with a large error can also be obtained, and this cannot be ignored. The main reason for the poor robustness is that the BP method easily falls into a local minimum. Because the initial network weight is set by the random assignment method, the phenomenon of falling into a local minimum is random and leads to the poor robustness of the BP method.

Compared to the BP method, the BPEL method has higher robustness and inversion accuracy. The superiority of the BPEL method could be attributed to three factors. (1) The ensemble learning technique was adopted. The characteristics of ensemble learning include the use of differentiated base learning to improve robustness and accuracy. The BPEL uses the BP method as the base learning and uses the initial network weight random assignment characteristics to form different base learning. In other words, the ensemble learning technique turned the disadvantage of the initial network weight random assignment into an advantage, thereby improving the robustness and accuracy of the BPEL method. (2) An ensemble strategy based on the minimum outlying degree was proposed. In the inversion results of ensemble learning (BP method), most of the results were correct and stable, and only a few were noise and scattered. The ensemble strategy based on the minimum outlying degree could remove outlier noise and maintain the most stable value as the output, which ensured the high robustness and accuracy of the BPEL method. (3) The BPEL method retained the advantage of excellent nonlinear fitting of the BP method. Because the base learning of the BPEL method is the BP method, the advantage of the BP method was inherited. Furthermore, the disadvantage of the BP method was resolved by the above measures. Therefore, the BPEL method exhibited excellent performance in bathymetry.

4.2 *Recommendations for the number of training samples for the BPEL method*

Both BPEL and BP methods have a high demand for training samples because both methods are statistical methods that directly train the inversion model by training samples. In this section, we discuss and provide recommendations for selecting the number of training samples, K.

Figure 11 shows that the RMSE of the bathymetric inversion initially rapidly decreases with increasing training samples K; after a certain value of K, the decrease in the RMSE becomes more gradual, and the RMSE value eventually stabilizes. This is because the mapping rules from MSI reflectance to water depth become increasingly clear and reliable as the number of training samples increases, causing the RMSE of the bathymetric inversion to rapidly decrease with increasing K. However, after the rules from training samples are mastered, further increases in training samples cannot exhibit new mapping rules, and the

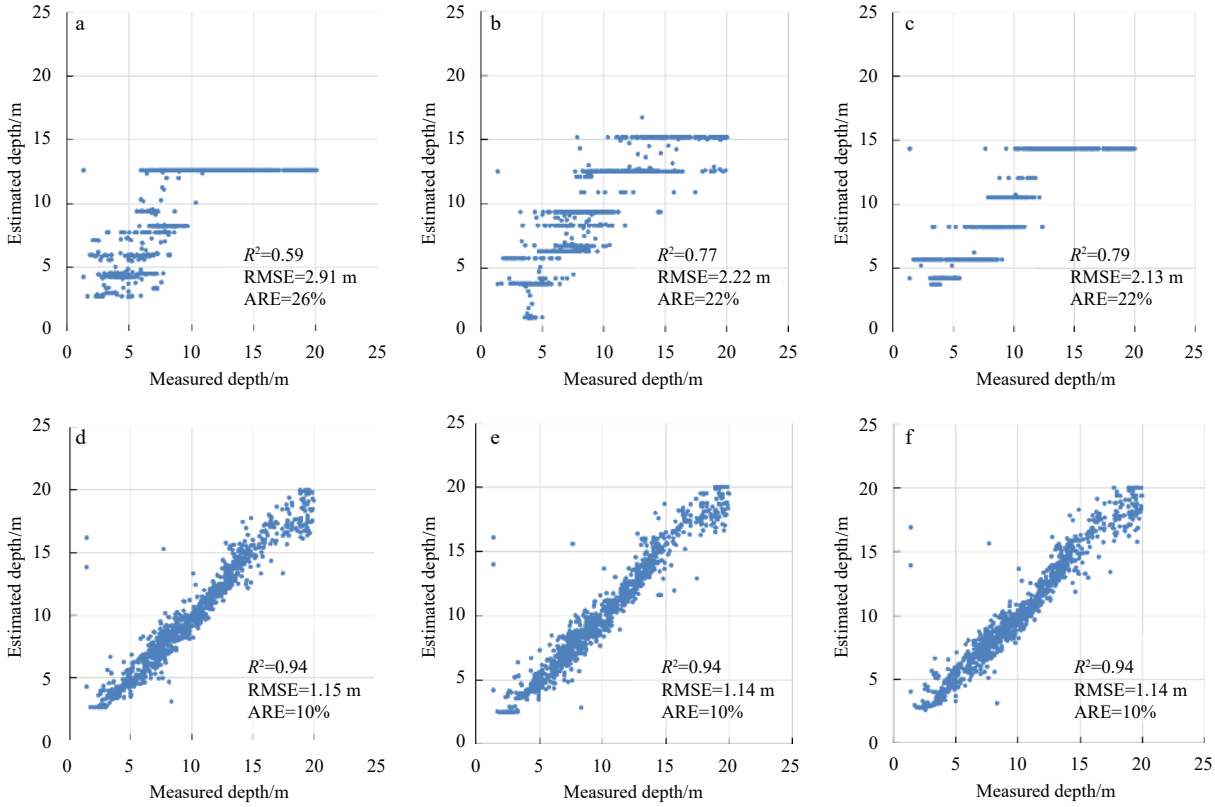

Fig. 6. Scatterplots (estimated depth versus measured depth) of the three worst results for the back propagation (BP) and BP neural network and ensemble learning (BPEL) methods in the Anda Reef. a–c. Scatterplots of the 85th, 31st, and 91st repeated experiments for the BP method. d–f. Scatterplots of the 50th, 70th, and 96th repeated experiments for the BPEL method.

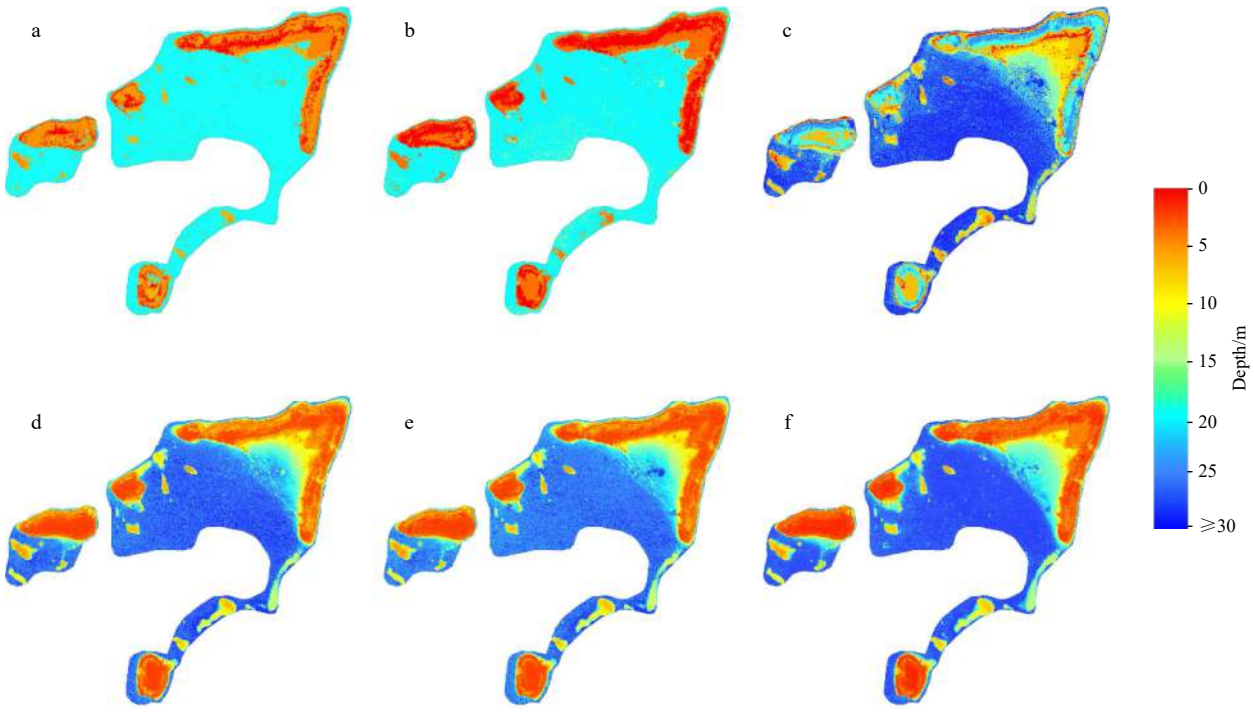

Fig. 7. Bathymetric maps of the three worst results for the back propagation (BP) and BP neural network and ensemble learning (BPEL) methods in the northeastern Jiuzhang Atoll. a–c. Bathymetric maps of the 57th, 72nd, and 91st repeated experiments for the BP method. d–f. Bathymetric maps of the 96th, 58th, and 8th repeated experiments for the BPEL method.

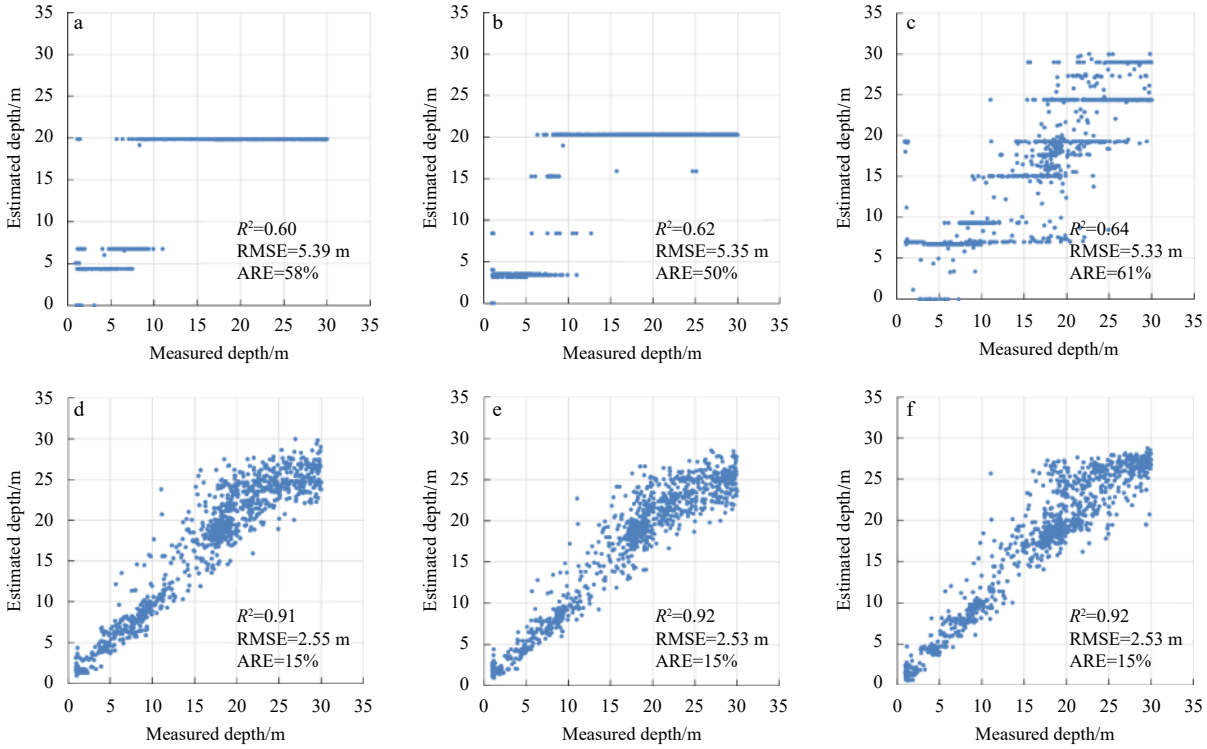

Fig. 8. Scatterplots (estimated depth versus measured depth) of the three worst results for the back propagation (BP) and BP neural network and ensemble learning (BPEL) methods in the northeastern Jiuzhang Atoll. a–c. Scatterplots of the 57th, 72nd, and 91st repeated experiments for the BP method. d–f. Scatterplots of the 96th, 58th, and 8th repeated experiments for the BPEL method.

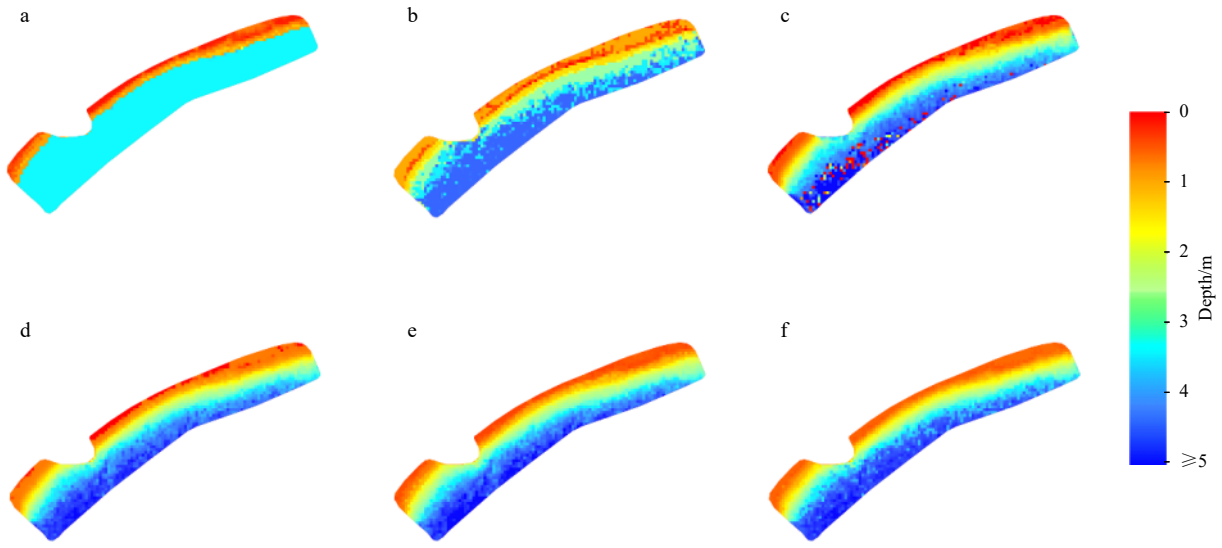

Fig. 9. Bathymetric maps of the three worst results for the back propagation (BP) and BP neural network and ensemble learning (BPEL) methods in the Pingtan coastal zone. a–c. Bathymetric maps of the 41st, 39th, and 45th repeated experiments for the BP method. d–f. Bathymetric maps of the 43rd, 74th, and 59th repeated experiments for the BPEL method.

RMSE is gradual. The number of training samples for the BPEL method can refer to the experience of the BP method because of their similar RMSE nodes from the decrease to stability (Fig. 11). In this experiment, it was found that K=200 was sufficient to achieve a high level of bathymetric accuracy. Hence, 200 training samples can be used as a reference value in other experiments. K can also be increased to ensure accuracy at the low and stable RMSEs region, based on the availability of sample data.

4.3 *Recommendations for the number of base learners for the BPEL method*

Compared with the BP method, the number of base learners, L, is a unique new parameter for the BPEL method. In this section, we discuss and provide recommendations for the selection of base learners, L.

In Fig. 12, it is shown that the RMSE and error bars are large when L=1 and L=2, and the RMSE and error bars are small when

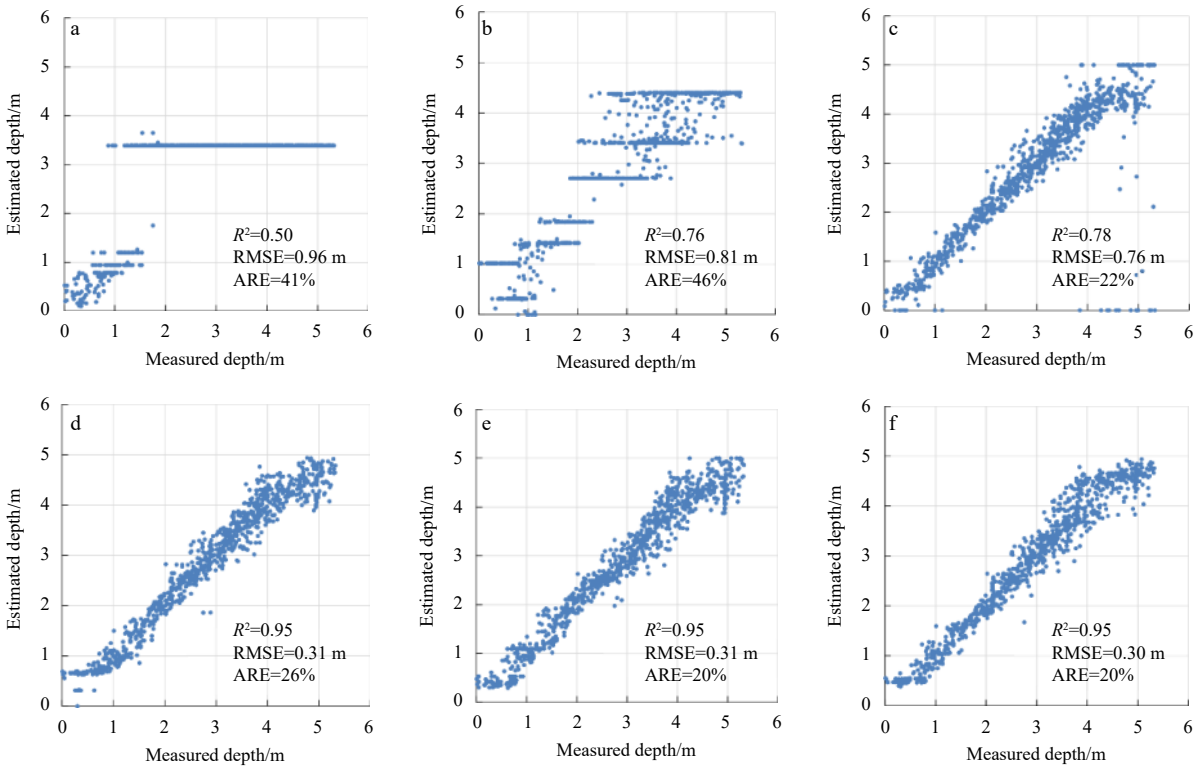

Fig. 10. Scatterplots (estimated depth versus measured depth) of the three worst results for the back propagation (BP) and BP neural network and ensemble learning (BPEL) methods in the Pingtan coastal zone. a–c. Scatterplots of the 41st, 39th, and 45th repeated experiments for the BP method. d–f. Scatterplots of the 43rd, 74th, and 59th repeated experiments for the BPEL method.

Table 1. Comparison of inversion accuracies (RMSEs) of the three worst results of the back propagation (BP) and BP neural network and ensemble learning (BPEL) methods

Study area	Water depth/m	*N*	BP			BPEL		
			Worst result	Second worst result	Third worst result	Worst result	Second worst result	Third worst result
Anda Reef	0–5	180	1.87	2.17	2.32	1.59	1.58	1.66
	5–10	386	2.99	1.96	1.33	0.92	0.93	0.88
	10–15	324	1.39	1.56	1.65	0.85	0.95	0.89
	15–20	125	5.41	3.56	3.76	1.35	1.20	1.31
	Overall	1 025	2.91	2.22	2.13	1.15	1.14	1.14
Northeastern Jiuzhang Atoll	0–5	150	5.07	2.73	10.09	0.84	0.77	0.85
	5–10	145	5.84	7.88	2.05	1.73	1.51	1.62
	10–15	73	7.54	7.79	4.02	3.26	2.98	3.42
	15–20	285	3.14	3.08	4.38	2.96	2.52	3.03
	20–25	187	2.98	2.67	4.4	2.27	2.04	2.62
	25–30	181	8.01	7.32	3.49	3.28	3.91	2.48
	Overall	1 021	5.39	5.35	5.33	2.55	2.53	2.53
Pingtan coastal zone	0–1	104	0.47	0.56	0.26	0.25	0.23	0.21
	1–2	135	1.44	0.47	0.29	0.20	0.22	0.15
	2–3	181	0.92	0.82	0.27	0.26	0.21	0.24
	3–4	256	0.37	0.69	0.39	0.27	0.31	0.35
	4–5	209	1.27	0.83	1.13	0.41	0.41	0.36
	Overall	885	0.96	0.81	0.76	0.31	0.31	0.30

Note: *N* represents the number of test samples.

$L \geqslant 3$. This can be explained as follows. When L=1, the RMSE and error bars of the BP method were displayed as a contrast. Because of the problem of the BP method easily falling into the local minimum, the RMSE and error bars are large. When L=2, the ensemble strategy based on the minimum outlying degree is ineffective because the inversion results from two base learners have the same outlying degree. The noise cannot be identified by the outlying degree; hence, the RMSE and error bars of the BPEL method are also large. When $L \geqslant 3$, the outlying degree of inversion from the base learners is different, and the ensemble strategy based on the minimum outlying degree can achieve superior noise removal performance. Therefore, $L \geqslant 3$ is necessary for the

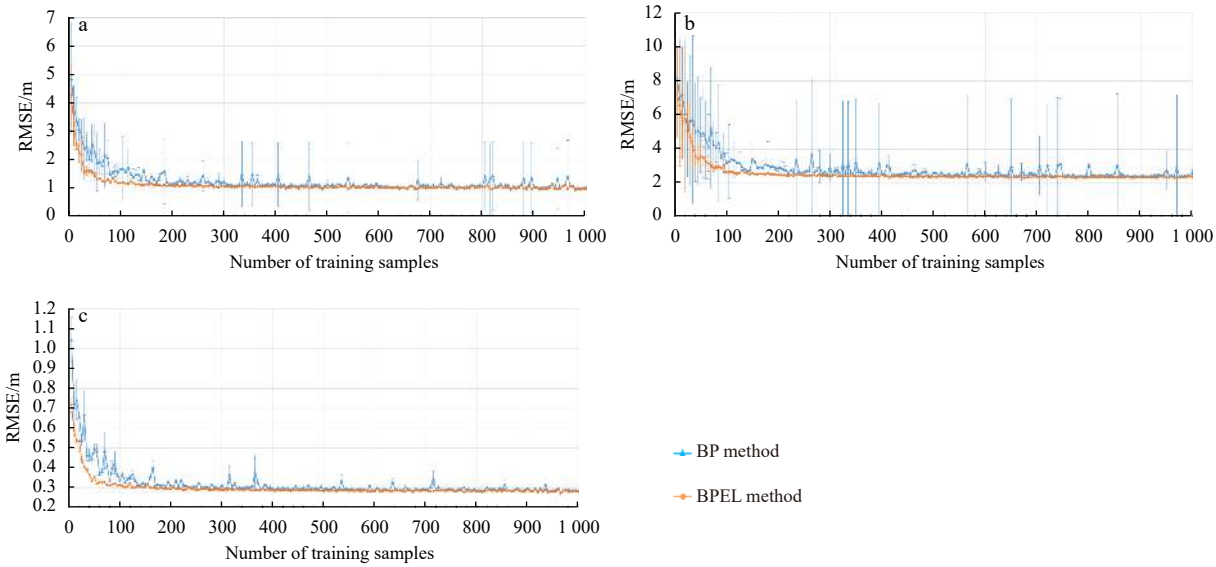

Fig. 11. Effects of the number of training samples on the accuracy of back propagation (BP) and BP neural network and ensemble learning (BPEL) methods. RMSE of bathymetric inversion experiments in the Anda Reef (a), northeastern Jiuzhang Atoll (b), and Pingtan coastal zone (c). Error bars are the standard deviation of the RMSE values.

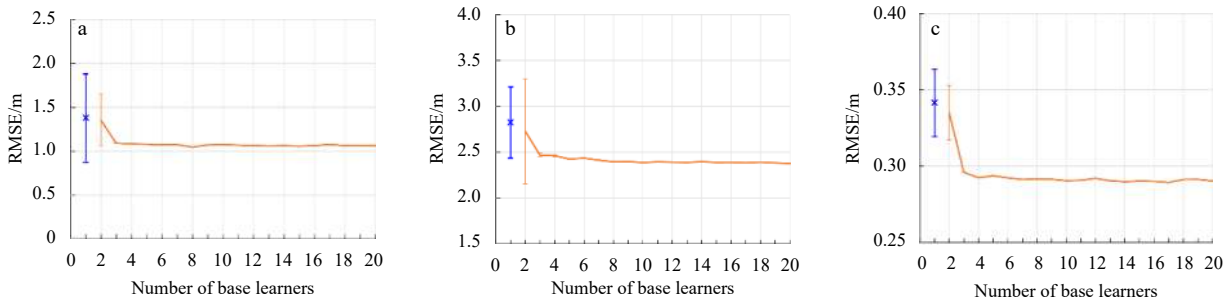

Fig. 12. Effects of the number of base learners on the accuracy of BP neural network and ensemble learning (BPEL) methods. RMSE of bathymetric inversion experiments in the Anda Reef (a), northeastern Jiuzhang Atoll (b), and Pingtan coastal zone (c). Error bars are the standard deviation of the RMSE values. The blue point and line in L=1 are the RMSE and error bar of the back propagation (BP) methods.

BPEL method.

5 Conclusions

This paper proposes a BPEL method that showed outstanding properties in bathymetric inversion in the Anda Reef, northeastern Jiuzhang Atoll, and Pingtan coastal zone. The following conclusions can be drawn from the experimental results.

(1) The new BPEL method can solve the poor robustness problem of the BP method, and obtain higher accuracy. Compared with the BP method, the RMSE and ARE of the BPEL method can reduce by 1.76 m and 16% in the Anda Reef experiment, reduce by 2.84 m and 46% in the northeastern Jiuzhang Atoll experiment, and reduce by 0.65 m and 26% in the Pingtan coastal zone experiment at most.

(2) The new ensemble strategy based on the minimum outlying degree can remove noise and retain optimum results, which ensures the high robustness and accuracy of the BPEL method.

(3) The optimal number of training samples (K) and number of base learners (L) are relatively stable and easily evaluated, which ensures high-quality bathymetric inversion. Furthermore, K=200 and the time-series length of $L \geqslant 3$ should be used as reference values in future BPEL experiments.

The proposed BPEL method has substantial potential in applications because it is relevant to all fields that use the BP method. Therefore, we will conduct application and extension research in the future.

References

Andréfouët S, Kramer P, Torres-Pulliza D, et al. 2003. Multi-site evaluation of IKONOS data for classification of tropical coral reef environments. Remote Sensing of Environment, 88(1–2): 128–143, doi: 10.1016/j.rse.2003.04.005

Andrejev O, Soomere T, Sokolov A, et al. 2011. The role of the spatial resolution of a three-dimensional hydrodynamic model for marine transport risk assessment. Oceanologia, 53(S1): 309–334, doi: 10.5697/oc.53-1-TI.309

Benardos P G, Vosniakos G C. 2007. Optimizing feedforward artificial neural network architecture. Engineering Applications of Artificial Intelligence, 20(3): 365–382, doi: 10.1016/j.engappai.2006.06.005

Cao Bincai, Fang Yong, Gao Li, et al. 2021. An active-passive fusion strategy and accuracy evaluation for shallow water bathymetry based on ICESat-2 ATLAS laser point cloud and satellite remote sensing imagery. International Journal of Remote Sensing, 42(8): 2783–2806, doi: 10.1080/01431161.2020.1862441

Casal G, Monteys X, Hedley J, et al. 2019. Assessment of empirical al-

gorithms for bathymetry extraction using Sentinel-2 data. International Journal of Remote Sensing, 40(8): 2855–2879, doi: 10.1080/01431161.2018.1533660

Ceyhun Ö, Yalçın A. 2010. Remote sensing of water depths in shallow waters via artificial neural networks. Estuarine, Coastal and Shelf Science, 89(1): 89–96, doi: 10.1016/j.ecss.2010.05.015

Chu Sensen, Cheng Liang, Ruan Xiaoguang, et al. 2019. Technical framework for shallow-water bathymetry with high reliability and no missing data based on time-series Sentinel-2 images. IEEE Transactions on Geoscience and Remote Sensing, 57(11): 8745–8763, doi: 10.1109/TGRS.2019.2922724

Collin A, Etienne S, Feunteun E. 2017. VHR coastal bathymetry using WorldView-3: colour versus learner. Remote Sensing Letters, 8(11): 1072–1081, doi: 10.1080/2150704X.2017.1354261

Deng Ying, Zhou Xiaoling, Shen Jiao, et al. 2021. New methods based on back propagation (BP) and radial basis function (RBF) artificial neural networks (ANNs) for predicting the occurrence of haloketones in tap water. Science of The Total Environment, 772: 145534, doi: 10.1016/j.scitotenv.2021.145534

El-Mewafi M, Salah M, Fawzi B. 2018. Assessment of optical satellite images for bathymetry estimation in shallow areas using artificial neural network model. Journal of Geographic Information System, 7(4): 99–106, doi: 10.5923/j.ajgis.20180704.01

Gholamalifard M, Kutser T, Esmaili-Sari A, et al. 2013. Remotely sensed empirical modeling of bathymetry in the southeastern Caspian Sea. Remote Sensing, 5(6): 2746–2762, doi: 10.3390/rs5062746

Guo Hengliang, Yang Hong, Qiao Baojin, et al. 2021. Multi-resolution satellite images bathymetry inversion of Bangda Co in the western Tibetan Plateau. International Journal of Remote Sensing, 42(21): 8077–8098, doi: 10.1080/01431161.2021.1970271

Hirose Y, Yamashita K, Hijiya S. 1991. Back-propagation algorithm which varies the number of hidden units. Neural Networks, 4(1): 61–66, doi: 10.1016/0893-6080(91)90032-Z

Huang Rongyong, Yu Kefu, Wang Yinghui, et al. 2017. Bathymetry of the coral reefs of Weizhou Island based on multispectral satellite images. Remote Sensing, 9(7): 750, doi: 10.3390/rs9070750

Hussein H M, Nadaoka K. 2017. Assessment of machine learning approaches for bathymetry mapping in shallow water environments using multispectral satellite images. International Journal of Geoinformatics, 13(2): 1–15

Islam M M, Yao Xin, Murase K. 2003. A constructive algorithm for training cooperative neural network ensembles. IEEE Transactions on Neural Networks, 14(4): 820–834, doi: 10.1109/TNN.2003.813832

Kim J S, Baek D, Seo II W, et al. 2019. Retrieving shallow stream bathymetry from UAV-assisted RGB imagery using a geospatial regression method. Geomorphology, 341: 102–114, doi: 10.1016/j.geomorph.2019.05.016

Lee Zhongping, Carder K L, Mobley C D, et al. 1998. Hyperspectral remote sensing for shallow waters. I. A semianalytical model. Applied Optics, 37(27): 6329–6338, doi: 10.1364/AO.37.006329

Lee Y, Oh S H, Kim M W. 1993. An analysis of premature saturation in back propagation learning. Neural Networks, 6(5): 719–728, doi: 10.1016/S0893-6080(05)80116-9

Leon J X, Cohen T J. 2012. An improved bathymetric model for the modern and Palaeo Lake Eyre. Geomorphology, 173–174: 69–79, doi: 10.1016/j.geomorph.2012.05.029

Li Jing, Cheng Jihang, Shi Jingyuan, et al. 2012. Brief introduction of back propagation (BP) neural network algorithm and its improvement. In: Jin D, Lin S, eds. Advances in Computer Science and Information Engineering. Berlin: Springer, 553–558, doi: 10.1007/978-3-642-30223-7_87

Liang Jian, Zhang Jie, Ma Yi. 2017. A spatial resolution effect analysis of remote sensing bathymetry. Acta Oceanologica Sinica, 36(7): 102–109, doi: 10.1007/s13131-017-1088-x

Liu Shan, Gao Yong, Zheng Wenfeng, et al. 2015. Performance of two neural network models in bathymetry. Remote Sensing Letters, 6(4): 321–330, doi: 10.1080/2150704X.2015.1034885

Liu Shan, Wang Lei, Liu Hongxing, et al. 2018. Deriving bathymetry from optical images with a localized neural network algorithm. IEEE Transactions on Geoscience and Remote Sensing, 56(9): 5334–5342, doi: 10.1109/TGRS.2018.2814012

Lyzenga D R. 1978. Passive remote sensing techniques for mapping water depth and bottom features. Applied Optics, 17(3): 379–383, doi: 10.1364/ao.17.000379

Lyzenga D R. 1985. Shallow-water bathymetry using combined lidar and passive multispectral scanner data. International Journal of Remote Sensing, 6(1): 115–125, doi: 10.1080/01431168508948428

Ma Yue, Xu Nan, Liu Zhen, et al. 2020. Satellite-derived bathymetry using the ICESat-2 lidar and sentinel-2 imagery datasets. Remote Sensing of Environment, 250: 112047, doi: 10.1016/j.rse.2020.112047

Manessa M D M, Kanno A, Sagawa T, et al. 2018. Simulation-based investigation of the generality of Lyzenga's multispectral bathymetry formula in Case-1 coral reef water. Estuarine, Coastal and Shelf Science, 200: 81–90, doi: 10.1016/j.ecss.2017.10.014

Melet A, Teatini P, Le Cozannet G, et al. 2020. Earth observations for monitoring marine coastal hazards and their drivers. Surveys in Geophysics, 41(6): 1489–1534, doi: 10.1007/s10712-020-09594-5

Polcyn F C. 1976. NASA/Cousteau ocean bathymetry experiment. NASA CR-ERIM 118500-l-F. Ann Arbor, MI: Environmental Research Institute of Michigan

Qiu Luo, Zhang Dexian, Huang Hao, et al. 2018. BP artificial neural network and its application based on LM algorithm. NeuroQuantology, 16(6): 598–605, doi: 10.14704/nq.2018.16.6.1566

Rumelhart D E, McClelland J L. 1986. Parallel Distributed Processing: Explorations in the Microstructure of Cognition. Cambridge, MA: MIT Press

Sandidge J C, Holyer R J. 1998. Coastal bathymetry from hyperspectral observations of water radiance. Remote Sensing of Environment, 65(3): 341–352, doi: 10.1016/S0034-4257(98)00043-1

Stumpf R P, Holderied K, Sinclair M. 2003. Determination of water depth with high-resolution satellite imagery over variable bottom types. Limnology and Oceanography, 48(1): 547–556, doi: 10.4319/lo.2003.48.1_part_2.0547

Sun Minxuan, Yu Linjun, Zhang Ping, et al. 2021. Coastal water bathymetry for critical zone management using regression tree models from Gaofen-6 imagery. Ocean & Coastal Management, 204: 105522, doi: 10.1016/j.ocecoaman.2021.105522

Wang Yanhong, Zhou Xinghua, Li Cong, et al. 2020. Bathymetry model based on spectral and spatial multifeatures of remote sensing image. IEEE Geoscience and Remote Sensing Letters, 17(1): 37–41, doi: 10.1109/LGRS.2019.2915122

Appendix

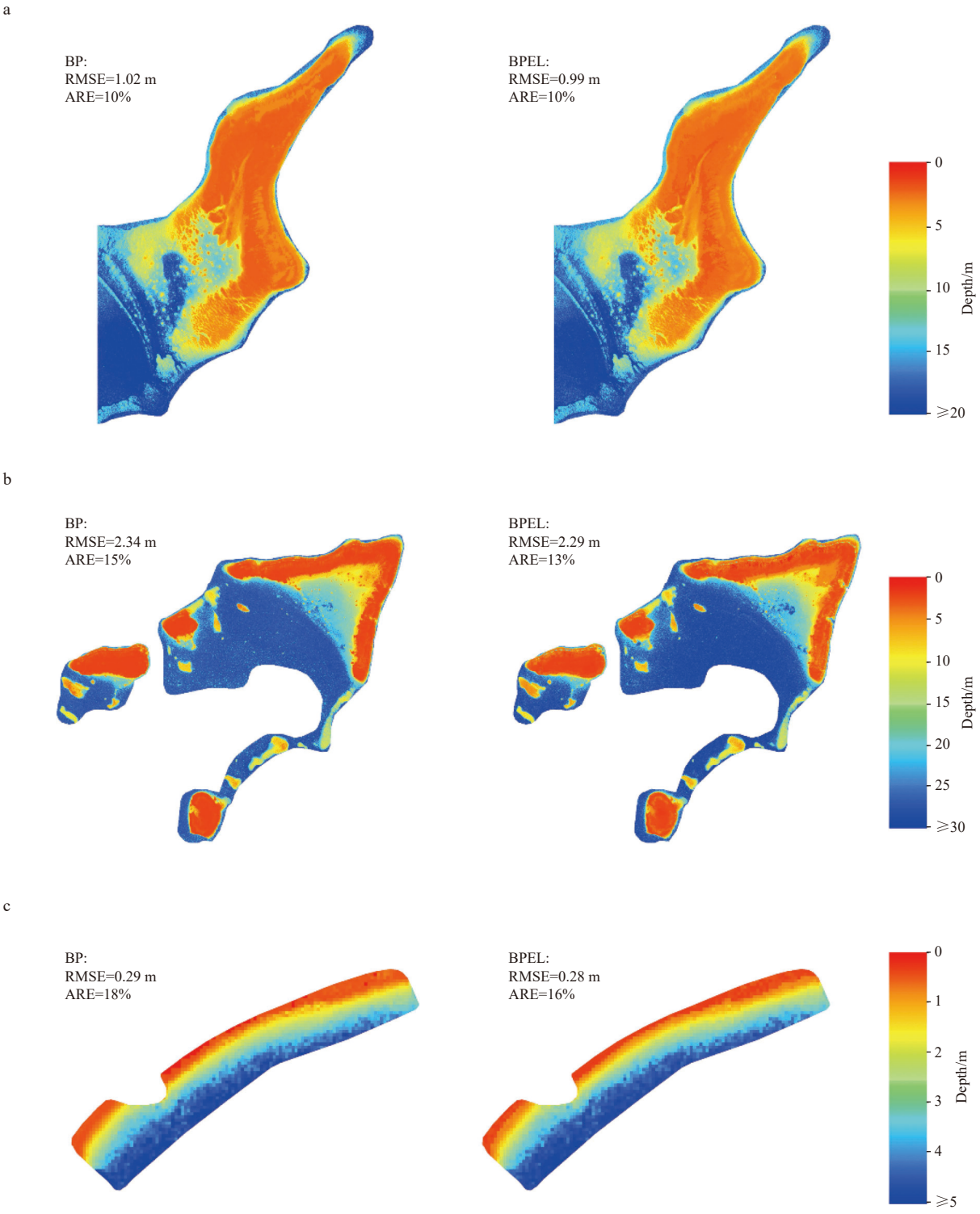

Fig. A1. Bathymetric maps of the best results for the back propagation (BP) and BP neural network and ensemble learning (BPEL) methods in the Anda Reef (a), northeastern Jiuzhang Atoll (b), and Pingtan coastal zone (c).